An investigation on the aerodynamics of a symmetrical airfoil in ground effect

M.R. Ahmed [a,*], S.D. Sharma [b]

[a] *Department of Engineering, The University of the South Pacific, Suva, Fiji*
[b] *Department of Aerospace Engineering, Indian Institute of Technology Bombay, Mumbai 400 076, India*

Abstract

The flow characteristics over a symmetrical airfoil—NACA 0015—are studied experimentally in a low speed wind tunnel. The pressure distribution on the airfoil surface was obtained, lift and drag forces were measured and mean velocity profiles were obtained over the surface. The wake region was also explored in detail and measurements of mean velocity and turbulence intensities were performed at two stations downstream of the trailing edge. Experiments were carried out by varying the angle of attack, α, from 0° to 10° and ground clearance of the trailing edge from the minimum possible value to one chord length. It was found that high values of pressure coefficient are obtained on the lower surface when the airfoil is close to the ground. This region of high pressure extended almost over the entire lower surface for higher angles of attack. As a result, higher values of lift coefficient are obtained when the airfoil is close to the ground. The flow accelerates over the airfoil due to flow diversion from the lower side, and a higher mean velocity is observed near the suction peak location. The pressure distribution on the upper surface did not change significantly with ground clearance for higher angles of attack. The upper surface suction causes an adverse pressure gradient especially for higher angles of attack, resulting in rapid decay of kinetic energy over the upper surface, leading to a thicker wake and higher turbulence level and hence a higher drag. The lift was found to drop at lower angles of attack at some values of ground clearance due to suction effect on the lower surface as the result of formation of a convergent–divergent passage between the airfoil and the ground plate. For the angle of attack of 12.5°, a very thick wake region was observed and higher values of turbulence intensity were recorded.

Keywords: Wing in ground effect (WIG); Aerodynamics; Hot-wire anemometry; Lift; Drag; Turbulence

1. Introduction

Favorable aerodynamic characteristics are obtained when a wing is in close proximity to ground. Works on development of Wing-in-Ground-effect (WIG) vehicles for large transport purpose can benefit immensely if the advantages of ground proximity are fully utilized. The effects of proximity to ground for an airfoil on the lift and drag characteristics were studied as early as in 1920s [1,2]. For small angles of attack, the lift force is found to increase with decreasing flight altitude. The flow around an airfoil or a wing is considerably modified under the influence of ground effect. The dividing streamline and the stagnation point move down, hence more air flows above the wing; thus there is a decrease in velocity and an increase in pressure below the wing. An air cushion is created by the high pressure that builds up under the wing when it is approaching the ground. For very small clearances, the air tends to stagnate under the wing, which will give the highest possible pressure,

Nomenclature

A	area of the airfoil ($=c \times$ span), mm^2	L	lift force, N
c	chord length, mm	p	static pressure, N/m^2
C_l	coefficient of lift ($= L/0.5\rho A U_\infty^2$), dimensionless	p_∞	freestream pressure, N/m^2
C_d	coefficient of drag ($= D/0.5\rho A U_\infty^2$), dimensionless	u	streamwise mean velocity, m/s
C_p	coefficient of pressure ($= [p - p_\infty]/0.5\rho U_\infty^2$), dimensionless	u_{rms}	RMS value of the fluctuations in u, m/s
D	drag force, N	U_∞	freestream mean velocity, m/s
h	height of trailing edge above the ground, mm	x	distance from the leading edge (along the chord), mm
l	distance from the trailing edge (axial), mm	y	vertical coordinate, mm
		α	angle of attack, degrees
		ρ	air density, kg/m^3

so called ram pressure. Simultaneously, the induced drag for a wing is lowered as the induced downwash velocity diminishes close to the ground. The streamline patterns over the leading and trailing edges of a wing in ground effect can be seen in ref. [3]. The streamline modification has interesting consequences—the effective angle of attack increases, resulting in an increase in lift force; on the other hand, the absence of downwash reduces the drag, which otherwise increases with angle of attack.

The L/D value is a measure of the efficiency of an aircraft [4] which can be expressed as the amount of power (thrust) that is required to propel an aircraft of a certain weight. Since thrust is equal to drag and weight is equal to lift in steady flight, this efficiency can be expressed as L/D. The increased lift and reduced drag obtained when the ground clearance is reduced, give much higher efficiency, which helps to increase the flight range at a reduced specific fuel consumption compared to the conventional aircraft. Besides, the WIG vehicle has other advantages over a conventional mode of air transport such as less energy consumption during take-off, no need of pressurized cabin, smaller infrastructure and safer runway as it is near the ground. The great potential of the WIG vehicles for possible application in both overwater and overland transport necessitates a thorough investigation of the flow characteristics over the wing.

2. Background

There have been some successful attempts to develop WIG vehicles that fly overwater. The initial success in the development of WIG vehicles was accomplished in Finland, Sweden and the United States. A review of the various types of vehicles experimented at various times is made by Ollila [5]. Ando [6] made a critical review of the design philosophies of overwater transport WIG vehicles. Work on development of overwater WIG vehicles is currently going on in many countries; the potential fuel savings and speed advantages over other modes of water transport providing the impetus.

A thorough investigation of the flow characteristics over the wings and other lifting surfaces is required from both practical and fundamental considerations. There have been some experimental as well as theoretical studies on influence of different wing configurations on the aerodynamic characteristics [7–19]. It has now been well documented that running in close to the ground gives increased lift force and studies have been performed both experimentally and numerically [7–14]. Studies performed by Ranzenbach and Barlow [12–14] demonstrated the ground effect for a single element airfoil configuration. They performed experiments and did numerical studies on single element symmetrical and cambered airfoils. They found that the lift force reaches a maximum at a ground clearance of approximately $0.08c$; beyond this the airfoil and ground boundary layers were found to merge, which was given as the explanation for reduced lift force very close to the ground. Although they documented the effect of ground proximity on the lift and drag forces, no other data were presented. Inviscid flow codes have been used for calculating the lift force. However, very close to the ground, these codes tend to give very high values of lift.

Ahmed and Kohama [15] presented results of an experimental investigation on a tandem wing configuration. They studied the influence of wing spacing in addition to the effects of angles of attack for the two wings and their ground clearances. Zhang et al. [16] reported the influence of tip vortex characteristics on the aerodynamic performance of a cambered airfoil. Zerihan and Zhang [17] reported pressure coefficient and lift and drag coefficient values on an airfoil provided with end plates. A flattened bottom surface was used to reduce the suction effect there. They found that at moderate clearances, separation of the boundary layer occurred near the trailing edge of the suction surface. The region

of separated flow was found to increase in size as the airfoil was brought very close to the ground. For an angle of attack of 1°, the flow was found to separate from the surface at about 0.7c for a ground clearance (h/c) of 0.067. They concluded that very close to the ground, the loss of lift force was due to a combination of flow separation and lower surface suction. Dominy (in [17]) postulated that in close proximity to ground, the wing stalls due to the adverse pressure gradient. In another paper, Zhang and Zerihan [18] investigated the wake behind a single element airfoil using laser anemometry. They found a thicker wake with reducing ground proximity as a result of boundary layer separation. Recently, Ahmed and Goonaratne [19] reported results of their measurements on a 17% thick wing for different angles of attack, ground clearances and flap angles. They observed increasing values of lift and drag coefficients with angle of attack. They also reported increasing lift coefficient values and decreasing drag coefficient values as the ground was approached for an angle of attack of 2° and different flap angles. Thus, it is clear that most of the studies are limited to force measurements. Some studies have involved surface pressure measurements and a few studies have explored wake and tip vortices. Detailed measurements of surface pressures, lift and drag forces, velocity distribution over the surface and wake survey for a variety of configurations to clearly understand the flow structure still need to be done.

The present paper deals with a study of the aerodynamic characteristics—pressure distribution on the surface of the airfoil, lift and drag coefficients, mean velocity distribution over the surface of the airfoil and mean velocity and turbulence intensity distributions in the wake region for a NACA 0015 airfoil for different angles of attack and for different ground clearances of the trailing edge.

3. Objectives

A survey of the literature shows that detailed studies of surface pressures, mean and fluctuating velocities over the surface and in the wake region of the wing alongwith lift and drag forces need to be carried out for different airfoil configurations. A justifiable need to test a standard NACA profile in close ground proximity was hence strongly felt. Although the present facility does not allow simulation of a very high Reynolds number, it was felt that useful data can be generated which can enhance our understanding of the ground effect phenomenon. Despite numerous research efforts being directed at the WIG phenomenon, complete understanding of the aerodynamics of ground effect is still lacking. Information on aerodynamic characteristics of different wing configurations in ground effect is also needed to help the designer choose the right profile for his application. The present work was undertaken with the aim of studying the influence of angle of attack and ground clearance of the trailing edge on an airfoil in context of a WIG vehicle and generating data for use of vehicle designer. The main objectives of the present work are: (a) to study the pressure distribution over the wing surface at different ground clearances and angles of attack and to measure the lift and drag forces and (b) to study the mean flow over the surface of the wing and to follow the flow in the wake region for mean and fluctuating velocities.

4. Experimental method

4.1. Wind tunnel

The experiments were carried out at a velocity of 35 m/s in an open circuit, suction type, low-speed wind tunnel. The air flow in the tunnel was generated by a single stage axial flow fan having a rated discharge of 216 m^3/min at the total pressure of 101.172 kPa and driven by a thyristor controlled 3.75 kW DC motor having a maximum speed of 2800 rpm. A smooth variation in velocity from 5 m/s to 40 m/s can be achieved in the test section having dimensions of 300 mm × 300 mm × 1000 mm. The test section is provided with perspex windows on both sides. A traversing mechanism is provided on top of the test section for moving the pitot tube and the hot-wire anemometer probe along its length. A settling chamber, provided with honeycomb gauges and four MS screens of 18, 30, 50 and 100 mesh, was used for correcting the flow. A bell-mouthed inlet section ensured smooth entry of the air to the settling chamber. The airflow was discharged into the test section through the square outlet of the contraction, having a width of 900 mm at the inlet. The area ratio of the contraction nozzle is 9:1. The freestream turbulence intensity in the test section at the above velocity was found to be 0.8%. A two-component load-cell system was used for measuring the lift and drag forces on the airfoil. The system gives digital output of the lift and drag forces in kgf; it was calibrated regularly for force measurements and its linearity was ensured in the range of interest. The calibration graphs were used for lift and drag calculations.

4.2. Mechanism for varying the ground clearance

To simulate the ground, a flat plate was used inside the test section and this plate was moved vertically to maintain the desired ground clearance of the airfoil. The length of the plate was 400 mm and it was as wide as the test section. The desired ground clearance was obtained by adjusting the lengths of the four rods supporting the plate from the four corners, as depicted in Fig. 1. Although the ground (plate) was fixed in the present

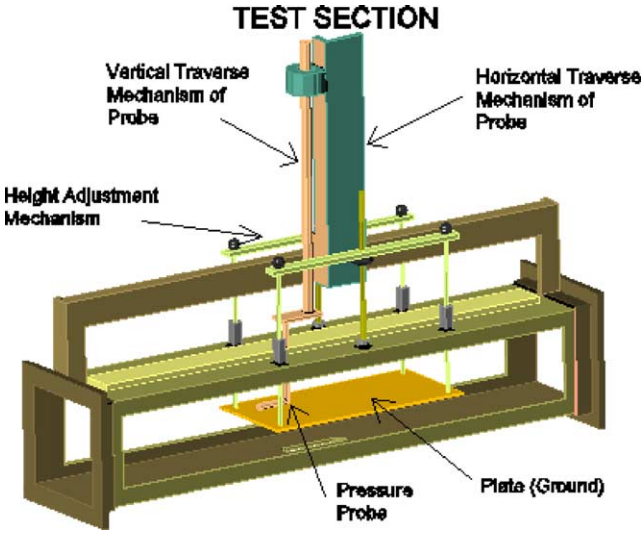

Fig. 1. A schematic diagram of the test section.

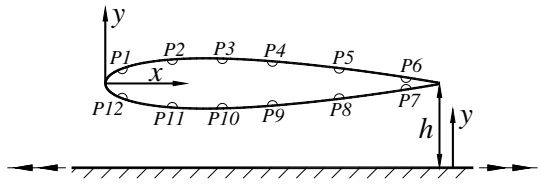

Fig. 2. Locations of pressure tappings.

investigation, every care was taken to simulate the true ground effect. An optimum length of the ground plate ahead of the airfoil was chosen to make sure that the boundary layer thickness was kept to a minimum without allowing streamlines to divert under the ground plate. Upstream of the airfoil, the ground plate length was slightly more than the chord length of the airfoil. Initial studies involving smoke injection were performed to make sure that at the angles of attack of interest, streamlines did not get diverted under the plate due to interference. The boundary layer thickness on the plate at the axial location of the leading edge of the airfoil was about 1 mm. As the chord length of the airfoil in the present studies is only 100 mm, it is expected that little error will be introduced due to stationary ground. It was found from measurements that both the plate and airfoil boundary layers are turbulent.

4.3. Test model and experimental set-up

The airfoil chosen for the present work was NACA 0015 (symmetric and having a maximum thickness of 15%). This profile was chosen as it is near this thickness that maximum lift coefficient is obtained [4]. The airfoil has a chord length of 100 mm and span of 300 mm, which is equal to the width of the test section, thus eliminating the third (spanwise) component and the wingtip vortices. In order to measure the pressure distribution on the airfoil surface, pressure taps were provided on both the sides, as shown in Fig. 2. The airfoil was mounted with the help of two pegs provided at the ends which exactly fitted into the holes provided on the two side windows of the test section.

With the help of a round protractor, the desired angle of attack for the airfoil was set. The airfoil was held at this angle using a screw mechanism. Measurements of surface pressure distribution were carried out with the help of a multibank water manometer to which all the tappings were connected. A slot was provided in the top wall of the test section for traversing the impact tube and the hot wire probe to measure the total pressure and the velocity respectively, at the desired location. A two component hot-wire anemometry system, consisting of two constant temperature anemometer (CTA) units, two signal conditioners, a mean value unit and an RMS unit, was used for the current investigation. The tungsten wire, used in the present investigation, has a diameter of 5 microns and a length of 2 mm. The test section blockage was checked at the maximum angle of attack of 10°. As the WIG craft fly at low angles of attack, most of the measurements such as those of lift and drag forces and velocity survey over the airfoil were limited to this angle of attack. A maximum blockage ratio of about 6% was found. A correction factor for the solid and wake blockage, ε, equal to a quarter of the ratio of the total frontal area and the test section area, was employed following ref. [19,20]. The freestream velocity in the test section, determined by the pitot tube was multiplied by $1 + \varepsilon$ to compensate for the total blockage effect [20]. The flow was found to separate from the surface for the angle of attack of 12.5° resulting in a thick wake region; hence, for this angle, only the wake region was explored and contours of mean velocity and turbulence intensity were plotted.

4.4. Experimental procedure

An impact tube was used for measuring the total pressure. The pressure was read at a U-tube water manometer as well as on a diaphragm type, digital pressure indicator. The static pressure was measured on the wall of the wind tunnel. For measuring the pressure at different points on the airfoil, a multi-tube manometer was used. The tubes were mounted on a board with adjustable inclination and were interconnected at the bottom with the balancing reservoir. The lift and drag measuring system was calibrated using standard weights.

The hot-wire anemometer was calibrated against the impact tube. All measurements in the present investigation were performed at a freestream mean velocity of 35 m/s. The Reynolds number, based on the corrected

velocity and the chord length of the airfoil, was 0.24×10^6.

The model was held in the test section at the desired angle of attack. The required velocity was set with the help of the thyristor speed control system. The readings from the multibank manometer were noted. The manometer board was set at an angle of 20° with the vertical for most of the pressure measurements. Experiments were performed by varying the angle of attack, α, from 0° to 10°. The ground clearance of the airfoil (h) was varied from the minimum possible value to 90 mm, giving h/c values of upto 0.9. For lower angles of attack, measurements at small values of h could not be performed as the thicker part of the airfoil was touching the ground plate. Thus, at the angle of attack of 0°, the minimum value of h obtained was 8.5 mm. Distributions of mean velocity were obtained over the surface of the airfoil to study the accelerated flow there. In the wake region, hot-wire probe was traversed from 3 mm above the plate to nearly 100 mm at two axial locations of 50 mm and 100 mm from the trailing edge of the airfoil model. For the angle of attack of 12.5°, the wake region was found to be much thicker and measurements were performed upto about 160 mm above the plate.

The accuracy of measurements of C_p was estimated by calculating dC_p from the expression for C_p (i.e. $C_p = [p - p_\infty]/0.5\rho U_\infty^2$). Thus, the measurements of C_p in the present studies were made with an accuracy of 1.8%. The accuracy of measurements of velocity was estimated following the procedure in ref. [21]. The accuracies of calibration and conversion (uncertainty related to curve-fitting errors) were taken into consideration for estimation of error. As the calibration was performed with the help of a Pitot tube, the maximum error in the measurement of velocity was estimated to be about 2.2%. The conversion accuracy was estimated to be within 1.5%. A large number of samples was acquired to reduce the uncertainty level of turbulence intensity measurements, following the procedure in ref. [21]. The uncertainty in the measurement of turbulence intensity was within 3.1%.

5. Results and discussion

The results are presented and discussed in this section. For calculation of C_p, the measured static pressure at a location was non-dimensionalized with respect to the freestream static pressure and the corrected freestream mean velocity (U_∞). All mean and fluctuating velocities were non-dimensionalized with respect to the corrected freestream mean velocity (U_∞).

5.1. Surface pressure distribution

Figs. 3–7 show the variation of Coefficient of Pressure (C_p) on the surface of the airfoil with ground clearance, for different angles of attack. Fig. 3 shows the variation in the pressure on the airfoil surface for the angle of attack, α, of 0° and different ground clearances.

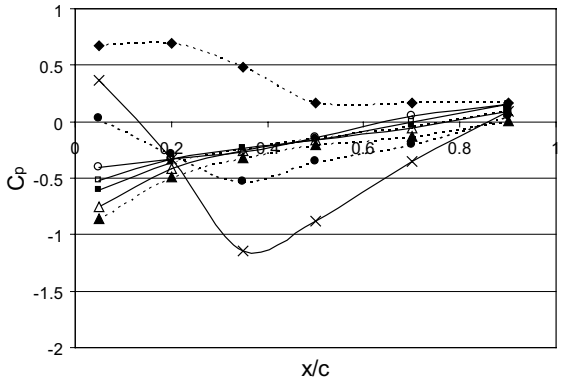

Fig. 3. Pressure distribution on the surface of the airfoil for an angle of attack of 0°. ♦ pr. side ▲ suction side for $h/c = 0.085$, × pr. side △ suction side for $h/c = 0.15$ ● pr. side ■ suction side for $h/c = 0.25$, ○ pr. side □ suction side for $h/c = 0.85$.

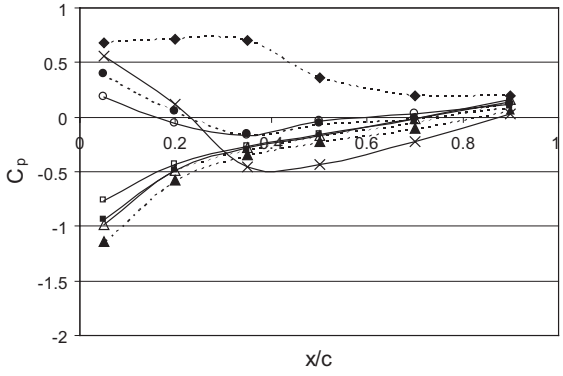

Fig. 4. Pressure distribution on the surface of the airfoil for an angle of attack of 2.5°. ♦ pr. side ▲ suction side for $h/c = 0.05$, × pr. side △ suction side for $h/c = 0.15$ ● pr. side ■ suction side for $h/c = 0.3$, ○ pr. side □ suction side for $h/c = 0.9$.

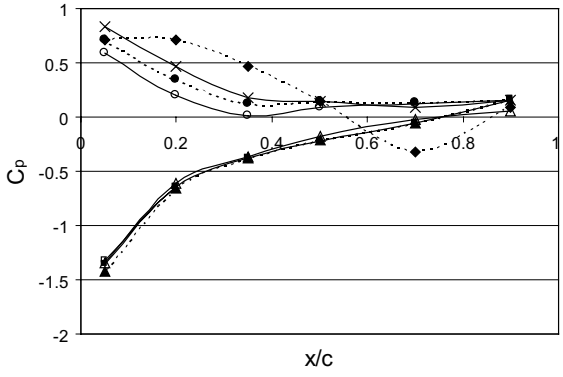

Fig. 5. Pressure distribution on the surface of the airfoil for an angle of attack of 5°. ♦ pr. side ▲ suction side for $h/c = 0.05$, × pr. side △ suction side for $h/c = 0.15$ ● pr. side ■ suction side for $h/c = 0.25$, ○ pr. side □ suction side for $h/c = 0.9$.

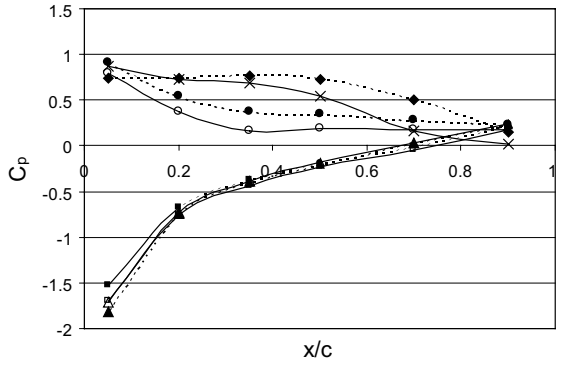

Fig. 6. Pressure distribution on the surface of the airfoil for an angle of attack of 7.5°. ♦ pr. side ▲ suction side for $h/c = 0.02$, × pr. side △ suction side for $h/c = 0.05$ ● pr. side ■ suction side for $h/c = 0.25$, ○ pr. side □ suction side for $h/c = 0.8$.

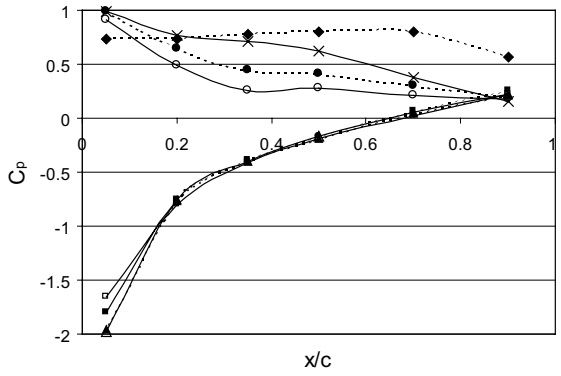

Fig. 7. Pressure distribution on the surface of the airfoil for an angle of attack of 10°. ♦ pr. side ▲ suction side for $h/c = 0.0$, × pr. side △ suction side for $h/c = 0.05$ ● pr. side ■ suction side for $h/c = 0.2$, ○ pr. side □ suction side for $h/c = 0.8$.

Due to the ramming action, the pressure is high on the lower surface at points close to the leading edge. For the smallest ground clearance, the pressure is high on the lower surface and positive at all the points. A very interesting observation in these measurements is a suction effect on the lower surface at ground clearances of $h/c = 0.1$ to $h/c = 0.25$, although the pressure is positive at the first measurement point. This is because the area between the airfoil and the ground plate forms a convergent–divergent passage, and its effect is more prominent for lower ground clearances. A few calculations of theoretical pressure were performed at different locations using continuity and Bernoulli's equations. The free-stream velocity was used to calculate the velocity under the wing at different locations. The pressure at the first measurement location was used as the reference pressure and from this, pressures at different points on the lower surface were estimated. Although the values did not match exactly (as it is difficult to correctly account for the loss of pressure due to friction), the general trend was found acceptable. The NACA 0015 section has maximum thickness at 29.3% of the chord, and at this location, the gap between the wing and the ground plate is minimum. This is the location where minimum pressure is expected. The nearest measurement location is at 35% of the chord length, and comparisons were made at this location. Pressures downstream of this location were always less than the pressures at the corresponding upstream locations, which can be attributed to the drop in pressure due to friction.

The pressure in the divergent zone increases sharply to meet the pressure on the upper surface near the trailing edge. Another interesting feature is the lower pressure at the last point compared to the points near the leading edge, due to the loss of pressure due to friction. This loss is higher when the value of h/c is small i.e. when the passage below the wing is smaller. For this angle of attack, a higher pressure at the first pressure tapping ($x/c = 0.05$) on the lower surface for lower values of h/c can clearly be seen.

As the ground clearance is increased, the value of C_p at the first location starts decreasing and at higher values of h/c, the value of C_p becomes negative at this location and does not show much variation with h/c. The figure shows the pressure distribution for the ground clearance of $h/c = 0.85$. For this ground clearance, the streamlines converge symmetrically on both sides of the airfoil, causing an increase in velocity on both the sides as there will be a reduction in pressure compared to the free-stream pressure, thus resulting in negative C_p values. The values of C_p on the first measurement location on both upper and lower surfaces become nearly the same for 0° angle of attack for higher ground clearances, which follows from the symmetry of the section on both sides of the chord line.

The values of C_p on the suction side in the absence of ground effect ($h/c = 0.8$ or 0.9) were compared with the theoretical values available in literature [22] to make sure that the relatively smaller test section did not cause increased acceleration or suction effect over the airfoil surface. It was found that generally the values of C_p on the upper surface are slightly higher (less negative) dispelling any doubts of upper wall interfering with the natural flow.

As the angle of attack is increased, higher values of C_p are observed on the lower surface and the region of high pressure extends towards the trailing edge. The pressure on the lower surface increases at $x/c = 0.05$ when the ground clearance is reduced, which indicates the shift of the stagnation point towards the bottom surface because of the ground effect. Simultaneously, there is a decrease in pressure on the suction side at $x/c = 0.05$ which indicates an increase in velocity over the airfoil because more air is forced to move over the upper surface due to ground effect. This increase in pressure on the pressure side and decrease in pressure on the suction side results in increase in the lift force.

Fig. 4 shows the pressure distribution on the surface of the airfoil for the angle of attack of 2.5° at ground clearances of $h/c = 0.05$, 0.15, 0.3 and 0.9. For the smallest ground clearance, the pressure coefficient is found to be positive at all the points on the lower surface, while a strong suction effect can be seen on the upper surface.

Higher increase in velocity over the surface is recorded at lower values of ground clearance, which is discussed in the next section. A suction effect on the lower surface due to the formation of a convergent–divergent path below the airfoil can clearly be seen from the figure for a ground clearance of $h/c = 0.15$. This effect was stronger for the angle of attack of 0°. Zerihan and Zhang [17] reported suction effect on the lower surface; however, they did not provide explanation for this. As the ground clearance is increased, the pressure on the lower surface as well as the suction effect on the upper surface decrease. A comparison of the pressure distributions for the smallest ground clearance ($h/c = 0.05$) and largest ground clearance ($h/c = 0.9$) clearly shows the effect of ground clearance on the flow over this airfoil; the high pressure on the lower surface completely disappears for the higher ground clearance and the suction effect on the upper surface also reduces.

There is a further increase in suction effect on the upper surface as the angle of attack is increased to 5°, as can be seen from Fig. 5 for a ground clearance of $h/c = 0.05$. For this angle of attack, the pressure on the lower surface is much higher at points near the trailing edge.

For a ground clearance of $h/c = 0.25$, the pressure coefficient is found to be positive at all the points on the lower surface. On the suction side, the pressure increases considerably from the leading edge for almost all angles of attack and all values of h/c, causing a reduction in velocity as the flow moves towards the trailing edge. For lower angles of attack, the reduction in velocity is small, as the flow divergence angle is not high, while for higher angles of attack, the reduction in velocity is considerable because of the high flow divergence angle, thus causing an adverse pressure gradient.

For the angles of attack of 7.5° and above, there is no divergent path under the wing and due to the ramming action, a very high value of C_p is recorded on the lower surface throughout the chord length of the airfoil. The C_p value at the first measurement location on the suction side is high negative (corresponding to the suction peak) and increases to a value of about 0.1 at the last measurement point close to the trailing edge, due to which there is a reduction in velocity towards the trailing edge. Fig. 6 shows the pressure distribution for this angle of attack at four values of ground clearance. It is interesting to see that the pressure distribution on the upper surface is not changing significantly with ground clearance. However, as we shall see in the next section, the lift force is higher at low ground clearances, which is mainly due to higher pressure on the lower surface. This high pressure region on the lower side grows towards the trailing edge with the increase in the angle of attack, as can be observed from a comparison of Figs. 4–7. The ramming effect is increasing with increase in angle of attack. The pressure on the lower surface is almost uniform (with a high value of C_p) all along the chord when the airfoil is in ground effect.

At the angle of attack of 10°, the values of C_p are very high on the pressure side for h/c values upto 0.15. For the h/c value of zero (trailing edge touching the plate), the value of C_p is close to one till trailing edge. For higher values of h/c, the value of C_p decreases towards the trailing edge (being nearly one at the first location of $x/c = 0.05$), as depicted in Fig. 7. As discussed earlier, a high suction is present at the first measurement location on the upper surface. For the angle of attack of 12.5°, a minimum C_p value of −2.2 was observed; however, the results of pressure distribution are not being presented here.

5.2. Lift and drag coefficients

Figs. 8 and 9 represent the lift and drag coefficients for the NACA 0015 airfoil for different angles of attack at varying ground clearances. The lift force was found to be higher for lower ground clearances. A maximum lift coefficient value of nearly 1.7 was measured for the angle of attack of 10° for no ground clearance of the airfoil, while for the maximum ground clearance of $h/c = 0.8$, a lift coefficient of nearly 1.0 was obtained. The results of the present measurements are in agreement with the previous studies on lift and drag forces [9,15,19]. The shape of the lift curve changes as the airfoil approaches the ground. It is interesting to note that the lift force reduces temporarily when the ground clearance (h/c) is about 0.2 for the angles of attack of 0° and 2.5°, due to the suction effect on the lower surface, discussed in the previous section. Zerihan and Zhang [17]

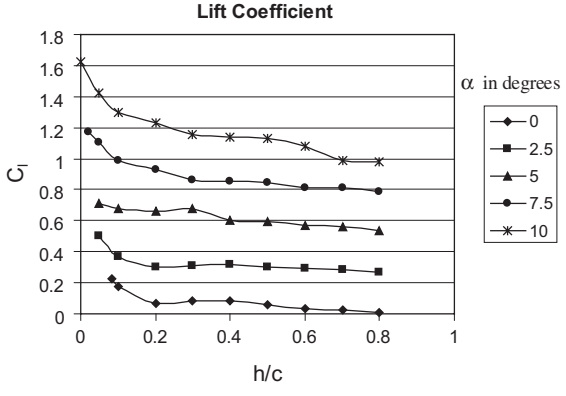

Fig. 8. Coefficient of lift at varying ground clearances for different angles of attack.

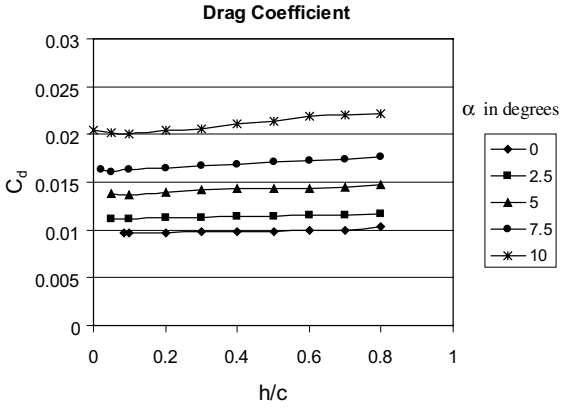

Fig. 9. Coefficient of drag at varying ground clearances for different angles of attack.

in their paper concluded that the lift force (downforce in their case, as the wing was inverted) reduces very close to the ground due to a combination of flow separation on the upper surface and suction effect on the lower surface. However, in the present work, the suction effect on the lower surface was found only at slightly higher ground clearances; hence, lift force was found to be higher for very low ground clearances. The suction effect on the lower surface can be reduced if a flatter surface at the bottom is used. For the angle of attack of 2.5°, the minimum value of C_p is not very low, hence there is less acceleration of flow over the airfoil surface. The high lift force at low ground clearances is thus mainly due to high pressure on the lower surface. The formation of convergent–divergent passage between the airfoil and the ground causes a significant drop in pressure on the lower surface for $h/c = 0.15$, which reduces the pressure difference between the lower and upper surfaces (Fig. 4), resulting in a lower lift force. A sharp dip in the lift force can be seen at $h/c = 0.2$; infact, the lift coefficient for $h/c = 0.2$ is less compared to $h/c = 0.4$ due to this. The results of drag measurements for different angles of attack and ground clearances are shown in Fig. 9. The drag force is seen to be essentially constant for the lower angles of attack of 0° and 2.5°. Similar observation was made by Ahmed and Goonaratne [19] for an angle of attack of 2°, with the drag coefficient increasing slightly with ground clearance.

For the angles of attack of 5° and higher, the drag coefficient was found to increase slightly with ground clearance. It can also be seen from the figure that for the lowest ground clearance, the drag coefficient is slightly higher. As we shall see in the following sections, the flow detaches from the upper surface before reaching the trailing edge forming a thick wake region, hence the contribution of pressure drag is found to be higher. However, as airfoil is a streamlined body, the influence of this increased pressure drag begins to be felt at higher angles of attack. As the three-dimensional effect of wing tip vortices is absent in the present case, the expected trend of continuously increasing drag coefficient with ground clearance was not observed. Fink et al. [in 23] reported essentially constant values of drag coefficient for angles of attack of 2.5° to 6.5° for a two-dimensional configuration. Detailed measurements of lift and drag coefficients for a 9% thick cambered airfoil were reported from the work of Chun et al. [in 23]. It was found that for an aspect ratio of 2, when the bottom of the end plates is lowered from the trailing edge by $0.1c$, the drag coefficient increased only slightly with ground clearance for angles of attack ranging from 0° to 8°. It is interesting to note that the values of both lift and drag coefficients reduce slightly as we slightly increase the ground clearance from the minimum value. For the lift coefficient, it is the suction effect on the lower surface and for the drag coefficient, it is the thinner wake which are responsible for this. The values of lift coefficients obtained in the present work for the case of $h/c = 0.8$ (minimum or no ground effect) are in good agreement with the values reported in the literature [24] for NACA 0015 section with no ground effect for a Reynolds number of 3.6×10^5, as shown in Table 1. The values for angles of attack of 2.5° and 7.5° were obtained by linear interpolation from the reported data. The values of drag coefficient in the present work were found to be slightly higher than the values reported in [24], which could partly be due to the difference in Reynolds number.

5.3. Velocity distribution over the airfoil

Distribution of mean velocity over the surface of the airfoil was plotted by making detailed measurements of velocity from (y=) 3 mm above the airfoil to about

Table 1
Comparison of the C_l and C_d values without ground effect from the present work with those of Sheldahl and Klimas [24]

Angle of attack (degrees)	Lift coefficient, C_l		Drag coefficient, C_d	
	Present work	Sheldahl and Klimas [24]	Present work	Sheldahl and Klimas [24]
0	0.01	0.0	0.0103	0.0091
2.5	0.265	0.27	0.0117	0.0096
5.0	0.54	0.55	0.0148	0.0114
7.5	0.788	0.7815	0.0176	0.0150
10.0	0.981	0.944	0.0222	0.0191

80 mm and (x=) 5 mm from the leading edge to 90 mm at values of ground clearance ranging from the minimum possible value of h/c for that particular angle of attack to $h/c = 0.5$ (as there was little influence of ground clearance on mean velocity over the surface at higher value of h/c). It should be noted that the distance y is measured from the airfoil surface for reporting velocity distribution over the airfoil surface and from the ground plate for wake measurements (please see Fig. 2). Measurements were not performed at $y = 1$ or 2 mm to avoid frequent breakage of the hot wire.

Fig. 10 shows the variation of mean velocity along the chord length of the airfoil for an angle of attack of 2.5° and a ground clearance (h/c) of 0.05. As can be seen from the figure, the flow accelerates over the airfoil and a mean velocity of $u/U_\infty = 1.3$ was recorded at $x/c = 0.05$; the flow velocity then continuously decreases towards the trailing edge. The flow was found to detach from the upper surface before the trailing edge for lower ground clearances; an observation which was earlier reported by Zerihan and Zhang [17,18] and was attributed to the adverse pressure gradient over the suction surface. It can be observed from Fig. 4 that the value of C_p is minimum at the first measurement location and the pressure rise is steepest for this ground clearance, which gives rise to flow detachment from the surface before the trailing edge. This results in a thick and highly turbulent wake, as will be seen in the following section. For a higher ground clearance of $h/c = 0.3$ for this angle (not shown), the pressure recovery is smaller, hence the flow remained attached to the upper surface till close to the trailing edge.

The distribution of mean velocity over the surface for an angle of attack of 7.5° and a ground clearance (h/c) of 0.02 is shown in Fig. 11. A considerably stronger suction effect on the upper surface (a C_p value of −1.81) gives rise to accelerated flow there. The flow has to overcome an adverse pressure gradient (can be seen from Fig. 6); hence the velocity reduces sharply to overcome this gradient.

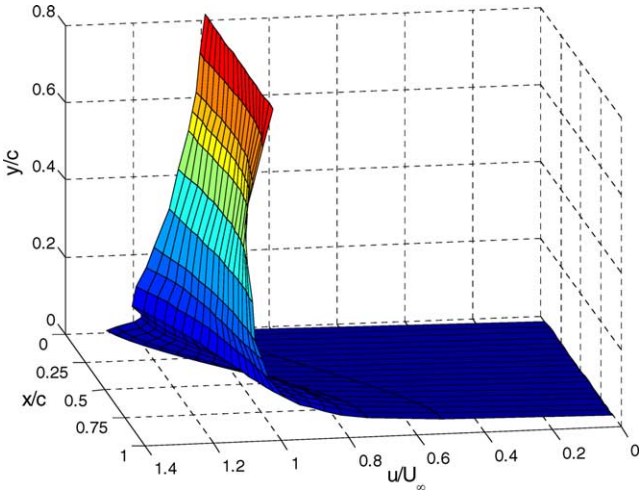

Fig. 11. Mean velocity distribution over the surface of the airfoil at $\alpha = 7.5°$ and ground clearance (h/c) of 0.02.

Fig. 12 shows the variation of velocity over the surface for an angle of attack of 10° and a ground clearance (h/c) of 0.1. The maximum measured velocity in this case is more than 1.4 i.e., an increase of more than 40% above the freestream mean velocity. Pressure measurements on the surface showed a high suction effect on the upper surface (not shown). It can be seen from Fig. 7 that maximum suction effect on the upper surface is obtained for this angle of attack. This causes the flow to be diverted above the airfoil, while below the airfoil, the flow nearly stagnates. Due to the high flow divergence angle over the surface in this case, the flow velocity reduces rapidly towards the trailing edge; a velocity

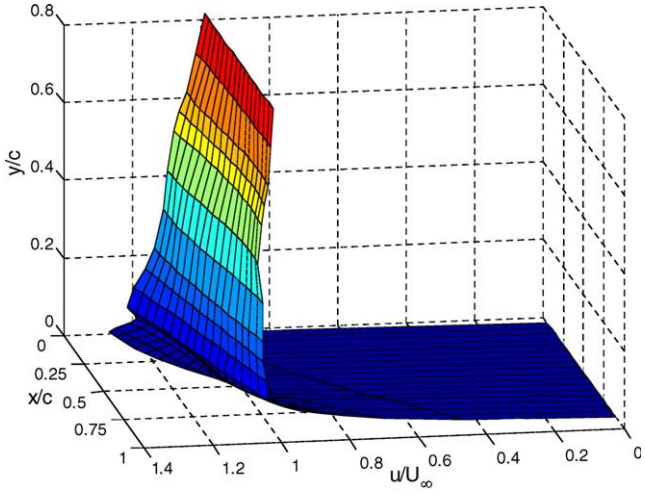

Fig. 10. Mean velocity distribution over the surface of the airfoil at $\alpha = 2.5°$ and ground clearance (h/c) of 0.05.

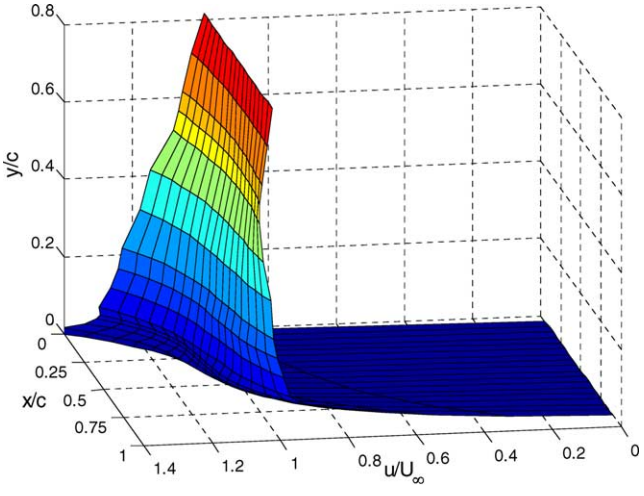

Fig. 12. Mean velocity distribution over the surface of the airfoil at $\alpha = 10°$ and ground clearance (h/c) of 0.1.

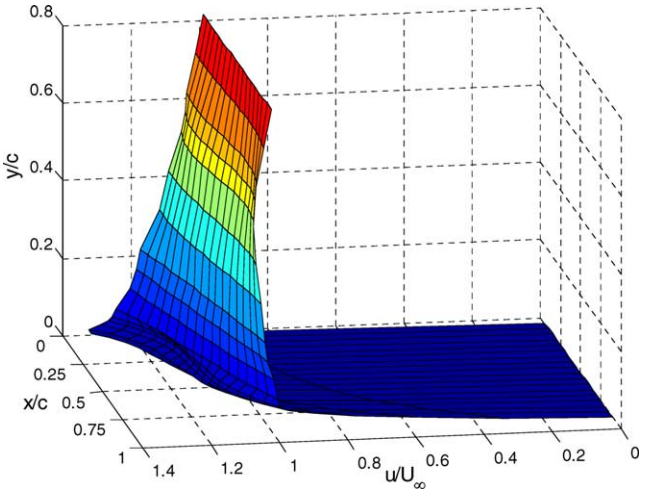

Fig. 13. Mean velocity distribution over the surface of the airfoil at $\alpha = 10°$ and ground clearance (h/c) of 0.3.

of 0.8 times the freestream velocity was observed at the location, $x/c = 0.75$. Similar observations have been made earlier and a detailed discussion on the suction effect over the airfoil surface and the associated accelerated flow can be found in [15]. The velocity further decreases downstream. A comparison of Figs. 10 and 12 makes it clear that for the higher angle, the presence of the airfoil affects the velocity field almost up to half the chord length distance in the vertical direction. The variation of mean velocity over the surface for an angle of attack of 10° and a ground clearance (h/c) of 0.3 is shown in Fig. 13. Clearly, for this case, the flow divergence over the airfoil and the deceleration towards the trailing edge are less.

5.4. Wake studies

In the wake region, measurements of mean velocity and turbulence intensity were performed at two axial locations—50 mm and 100 mm from the trailing edge (which correspond to $0.5c$ and $1.0c$ respectively). Measurements were made at values of ground clearance ranging from the minimum possible value of h/c for that particular angle of attack to $h/c = 0.5$, from 3 mm above the ground plate to about 100 mm; however for the angle of attack of 12.5°, measurements were performed upto $y/c = 1.8$ as the wake region was found to be considerably thicker for this angle of attack. Measurements were made at 4–5 values of ground clearance; however, only few results are being presented in this paper.

Figs. 14–22 show distributions of mean velocity and turbulence intensity in the wake region. It can be noted that the maximum defect in velocity profile and the peak in turbulence intensity correspond to approximately the height equal to the ground clearance of the airfoil.

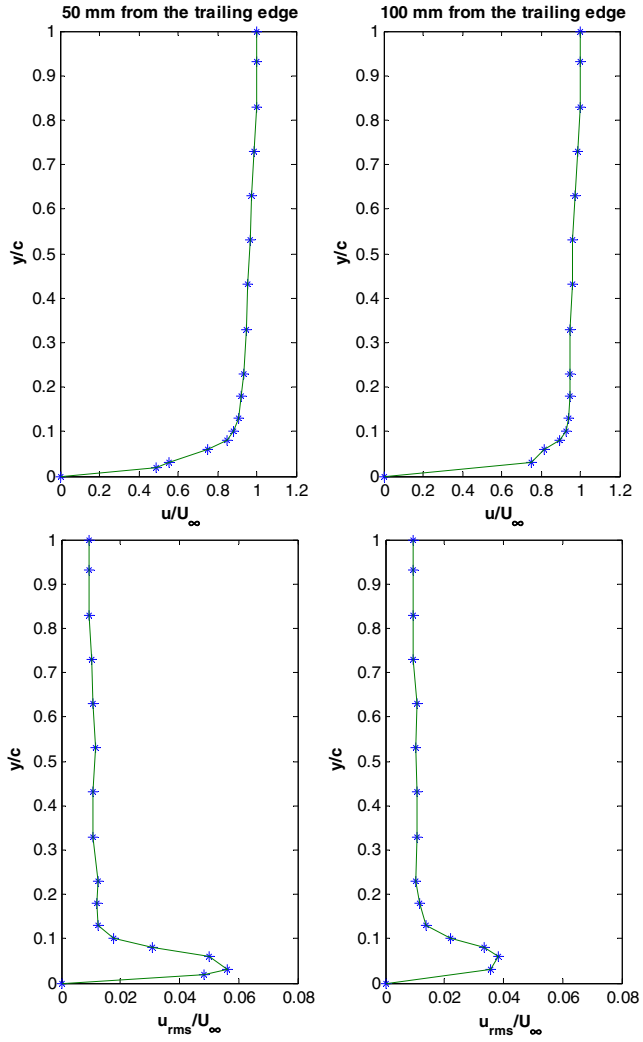

Fig. 14. Distributions of mean velocity and streamwise turbulence intensity in the wake region of the airfoil for $\alpha = 2.5°$ and ground clearance (h/c) of 0.05.

Fig. 14 shows the distributions of mean velocity and turbulence intensity in the wake region for an angle of attack of 2.5° at a ground clearance (h/c) of 0.05. The wake region is thicker for this case due to flow detachment before the trailing edge, resulting in a higher value of drag coefficient. The drag coefficient for this ground clearance is equal to the case of $h/c = 0.1$ (Fig. 9).

Fig. 15 shows the variations of mean velocity and turbulence intensity for a ground clearance of $h/c = 0.3$ for this angle of attack. The maximum turbulence level is only about 3% for this case, as compared to the lower ground clearance where it was nearly 6%. Another smaller peak in turbulence intensity profile corresponding to the plate boundary layer can be observed from this figure. The profiles of both the mean velocity and the turbulence intensity at the downstream location (100 mm from the trailing edge) become flatter.

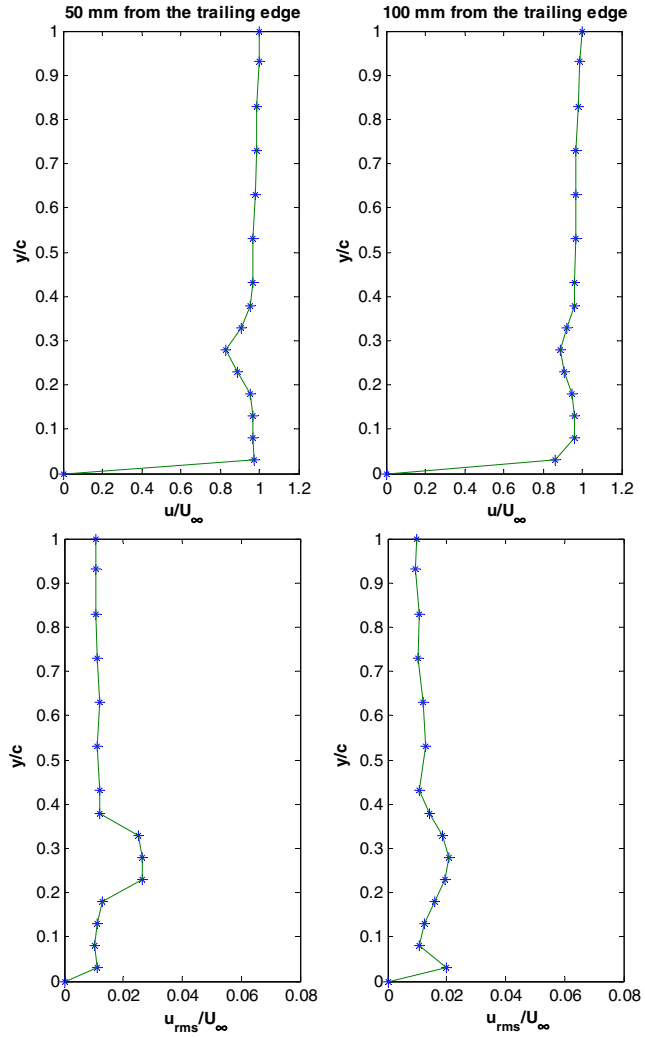

Fig. 15. Distributions of mean velocity and streamwise turbulence intensity in the wake region of the airfoil for $\alpha = 2.5°$ and ground clearance (h/c) of 0.3.

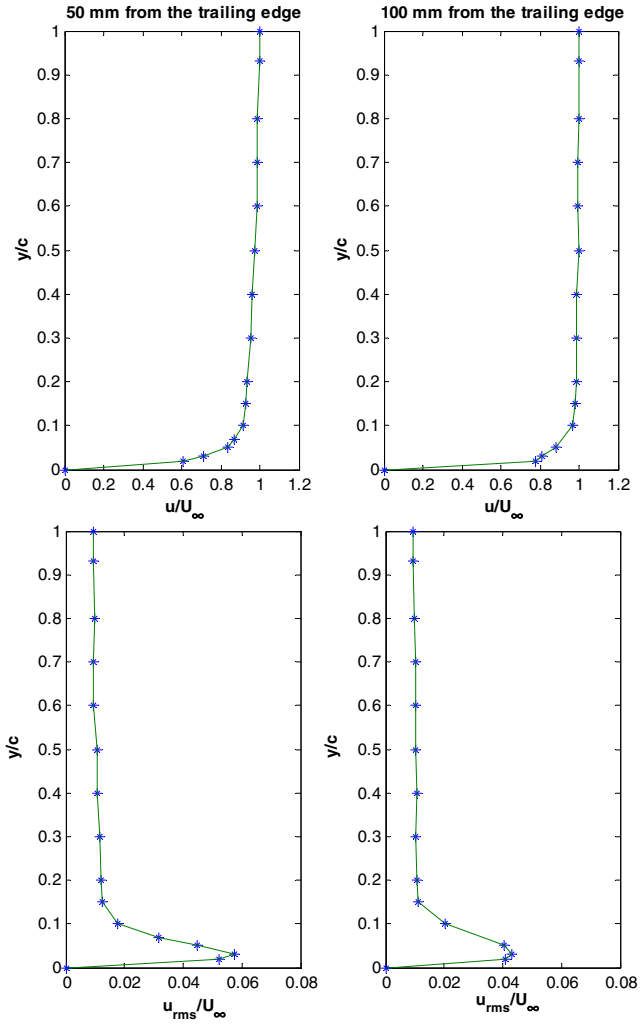

Fig. 16. Distributions of mean velocity and streamwise turbulence intensity in the wake region of the airfoil for $\alpha = 5°$ and ground clearance (h/c) of 0.035.

A larger defect in mean velocity profile and higher turbulence level can be seen from Fig. 16 for the angle of attack of 5° and a ground clearance of $h/c = 0.035$, as a result of flow detachment before the trailing edge, resulting in a relatively higher drag (Fig. 9). It can be seen from a comparison of Figs. 16 and 17 that when the airfoil is away from the ground, two distinct shear regions are present. When the airfoil is brought close to the ground, the two regions merge. Measurements by Ranzenbach and Barlow [12] and Zhang and Zerihan [18] in the wake region yielded similar results. Ranzenbach and Barlow [12] provided this as the explanation for lower lift forces close to the ground.

It is interesting to see that the drag force is higher for the lowest ground clearance of $h/c = 0.035$ compared to when $h/c = 0.1$ (Fig. 9). As can be seen from the profiles in Fig. 17, the wake is thinner and turbulence intensity is lower for the case when $h/c = 0.1$. The peaks in turbulence intensity due to the two shear regions are merged, with a higher turbulence intensity upto a height of $y/c = 0.2$.

For the angle of attack of 7.5° and a ground clearance of $h/c = 0.02$, there is a thicker region of shear flow over the airfoil due to flow divergence and the adverse pressure gradient to be overcome. As was shown in Fig. 6, the pressure rises considerably on the upper surface along the chord length from the suction peak. As the flow tries to overcome this adverse pressure gradient, it loses its kinetic energy. A drop in velocity (u/U_∞) from about 1.3 at $x/c = 0.05$ to less than 1 at $x/c = 0.35$, depicted in Fig. 11, is a clear indication of the effect of pressure gradient. When this low energy flow exits the airfoil, it forms a thick wake region with a high turbulence level, as can be seen from Fig. 18. The airfoil and the ground plate boundary layers are merged which causes a higher momentum loss for higher angles of

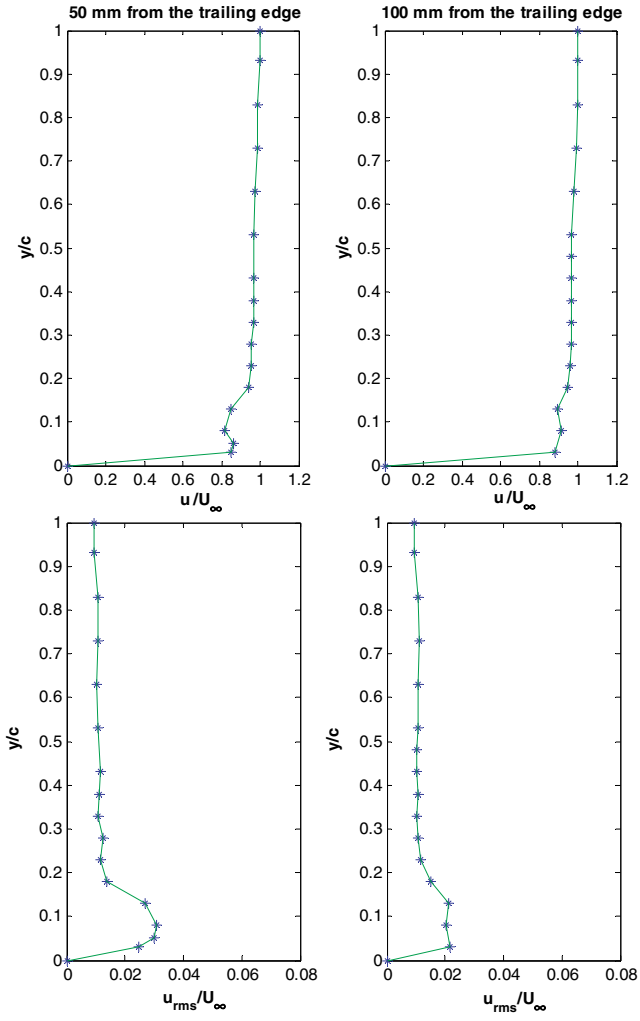

Fig. 17. Distributions of mean velocity and streamwise turbulence intensity in the wake region of the airfoil for $\alpha = 5°$ and ground clearance (h/c) of 0.1.

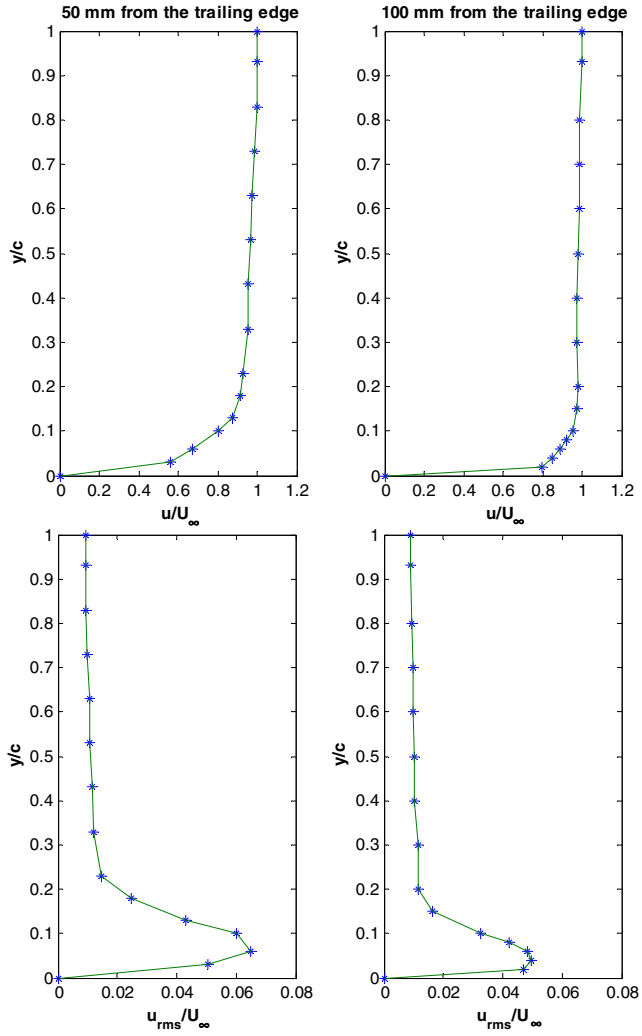

Fig. 18. Distributions of mean velocity and streamwise turbulence intensity in the wake region of the airfoil for $\alpha = 7.5°$ and ground clearance (h/c) of 0.02.

attack. The resulting high drag coefficient for this ground clearance can be seen from Fig. 9. It is interesting to see that the drag coefficient for this case is higher than for $h/c = 0.05$. Zerihan and Zhang [17] also reported higher values of drag for very small ground clearances. The lift force is still high for this case (Fig. 8) as the pressure is uniformly high on the lower surface (shown in Fig. 6). It is interesting to see that the change in lift force is mainly due to modification of lower surface pressure distribution. The shear region extends to slightly above $y/c = 0.2$.

A large defect in mean velocity profile and higher turbulence level are observed at the higher angle of attack of 10°, as can be seen from Fig. 19. The wake region is thicker than that for the lower angles of attack. At lower ground clearances, the velocity defect is larger due to the low kinetic energy flow leaving the surface before the trailing edge, resulting in a slightly higher drag (Fig. 9). The wake region shifts to higher y/c, as the ground clearance is increased. A turbulence level of more than 7% is observed at smaller values of ground clearance. The spreading of the shear region can be seen as the flow moves downstream. For higher value of h/c (not shown in the present paper), there are two distinct regions of velocity defect; one due to the wake of the airfoil and the other due to the ground plate boundary layer. For values of ground clearance of about 0.1, the boundary layer is penetrated by the accelerating stream, and hence the defect in velocity is not very large (can be seen from Fig. 17 for angle of attack of 5°), causing a drop in drag, depicted in Fig. 9. The spreading of the high turbulence region can also be seen from the figure. For a ground clearance of $h/c = 0.05$ for the angle of attack of 10°, a slight distinction between the two shear regions can be made from the velocity and turbulence profiles at the first location. As the passage under the wing acts like a nozzle for this angle, the velocity defect is not large, which is the reason for the slightly lesser

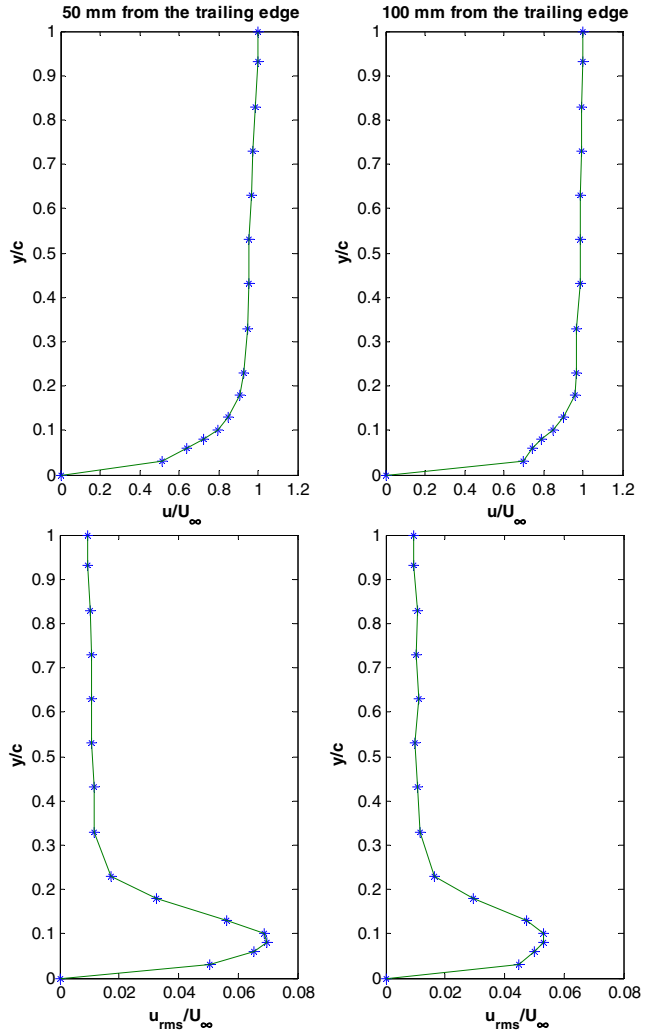

Fig. 19. Distributions of mean velocity and streamwise turbulence intensity in the wake region of the airfoil for $\alpha = 10°$ and ground clearance (h/c) of 0.012.

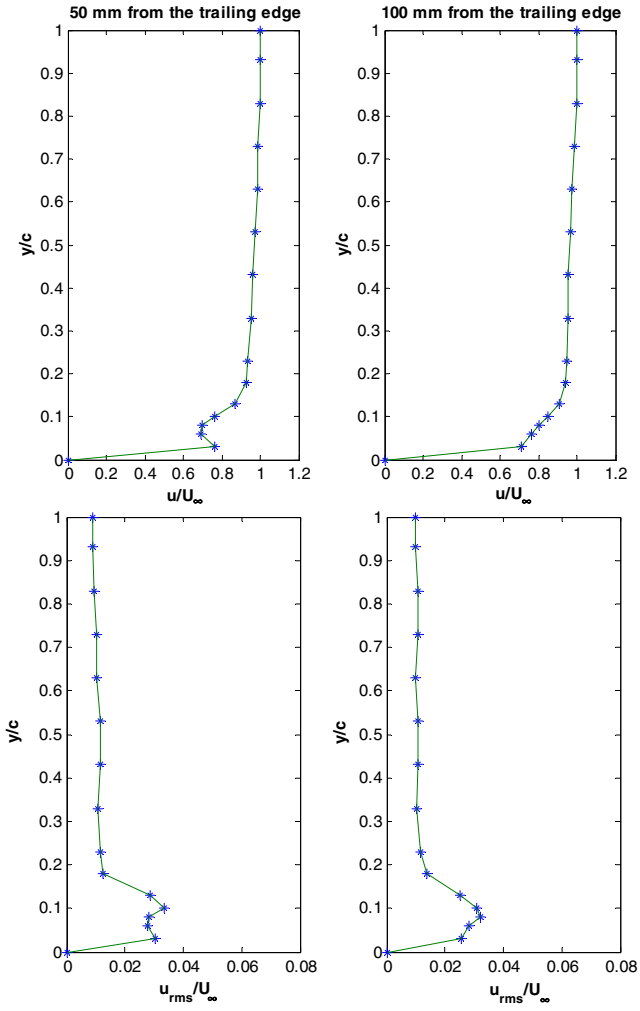

Fig. 20. Distributions of mean velocity and streamwise turbulence intensity in the wake region of the airfoil for $\alpha = 10°$ and ground clearance (h/c) of 0.05.

drag for this case. The two shear regions merge as we move downstream to a location of $l/c = 1.0$, as can be seen from Fig. 20.

The distribution of mean velocity and turbulence intensity for the angle of attack 12.5° at the wake location $l/c = 1.0$ are shown in three-dimensional form in Figs. 21 and 22. A considerably larger defect in mean velocity profile can be seen from Fig. 21. The wake region becomes very thick compared to smaller angles; hence measurements were performed upto a higher value of y/c. Fig. 22 shows the distribution of turbulence intensity for this case. Very high levels of turbulence intensity are observed for this angle of attack as the wake region is very thick due to early separation. The airfoil may stall at this angle of attack. The shifting of the velocity defect region and the turbulence intensity peak away from the ground, as the ground clearance is increased, can clearly be observed from this figure.

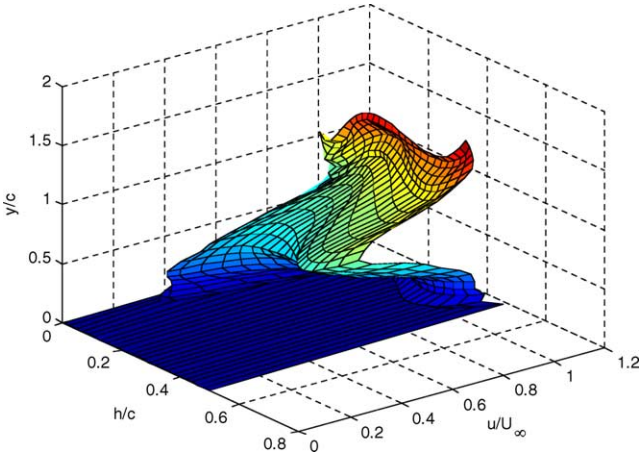

Fig. 21. Mean velocity distribution in the wake region of the airfoil at $\alpha = 12.5°$ and distance (l/c) of 1.0.

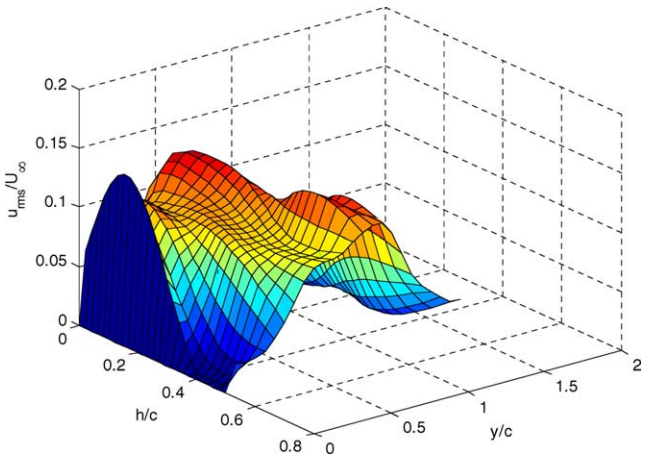

Fig. 22. Streamwise turbulence intensity distribution in the wake region of the airfoil at $\alpha = 12.5°$ and distance (l/c) of 1.0.

6. Conclusions

In the present work, a detailed investigation of the aerodynamic characteristics of NACA 0015 airfoil at different ground clearances was carried out. It was found from the experiments that both—the angle of attack and the ground clearance of the airfoil have a strong influence on the aerodynamic characteristics of the configuration. The important conclusions from the present work are:

1. A suction effect is observed on the lower surface at certain ground clearances at angles of attack upto 5°, due to the formation of a convergent–divergent passage between the airfoil and the ground, causing a local drop in lift force.
2. For very low ground clearances, the lift force was found to be always high, due to higher pressure on the lower surface of the airfoil. At higher angles of attack, high values of pressure coefficient were recorded on the lower surface with the high pressure region extending almost till the trailing edge of the airfoil, which resulted in higher lift force. The pressure distribution on the upper surface did not show significant variation with ground clearance, especially for higher angles of attack; hence, the higher lift force was mainly due to modification of pressure distribution on the lower surface.
3. A reduction in pressure on the suction side was observed at higher angles of attack, causing an adverse pressure gradient on the upper surface, a retarded flow and hence a thick wake region. At very low ground clearances, the airfoil and the ground plate boundary layers were found to merge which resulted in a higher momentum loss and hence a relatively higher drag for higher angles of attack.
4. For the angle of attack of 12.5°, the flow was found to separate from the surface very early, resulting in a thick and highly turbulent wake region.

7. Recommendations for future work

In the present work, a relatively thick symmetrical airfoil was tested in a low speed wind tunnel. Extensive measurements of all aerodynamic parameters are performed. The authors have performed studies on influence of camber on the aerodynamic characteristics [25]. However, extensive measurements on the aerodynamic characteristics of different airfoil sections over a wide range of Reynolds numbers are needed. This will help in generating a database which can be used for making a mathematical model. This can provide data to a WIG designer at the required Reynolds number.

Acknowledgment

Full financial support for the work reported here was received from Aeronautics R&D Board, Ministry of Defense, Govt. of India, under project No. Aero/RD-134/100/10/2000-2001/1108.

References

[1] A.E. Raymond, Ground influence on airfoils, NACA Technical Note 67, 1921.
[2] E.G. Reid, A full scale investigation of ground effect, NACA Technical Report 265, 1927.
[3] K.V. Rozhdestvensky, Aerodynamics of a Lifting System in Extreme Ground Effect, 1st ed., Springer-Verlag, 2000, p. 30.
[4] J.D. Anderson Jr., Fundamentals of Aerodynamics, third ed., McGraw-Hill, 2001, p. 283, 284, 334, 335.
[5] R.G. Ollila, Historical review of WIG vehicles, J. Hydronaut. 14 (3) (1980) 65–76.
[6] S. Ando, Critical review of design philosophies for recent transport WIG effect vehicles, Trans. Jpn Soc. Aeronaut. Space Sci. 33 (99) (1990) 28–40.
[7] A.W. Ailor, W.R. Eberle, Configuration effects on the lift of a body in close ground proximity, J. Aircraft 13 (8) (1976) 584–589.
[8] M.D. Chawla, L.C. Edwards, M.E. Frande, Wind-tunnel investigation of wing-in-ground effects, J. Aircraft 27 (4) (1990) 289–293.
[9] H. Tomaru, Y. Kohama, Experiments on wing in ground effect with fixed ground plate, in: Proceedings of the second JSME-KSME Fluids Engineering Conference, 1990, pp. 370–373.
[10] C.M. Hsiun, C.K. Chen, Aerodynamic characteristics of a two-dimensional airfoil with ground effect, J. Aircraft 33 (2) (1996) 386–392.
[11] H.H. Chun, I.R. Park, K.H. Chung, Computational and experimental studies on wings in ground effect and a wig effect craft, in: Proceedings of the Workshop on Ekranoplans and Very Fast Craft, University of New South Wales, 1996, pp. 38–59.
[12] R. Ranzenbach, J.B. Barlow, Two-dimensional airfoil in ground effect, an experimental and computational study, Society of Automotive Paper No. 94-2509, 1994.

[13] R. Ranzenbach, J.B. Barlow, Cambered aerofoil in ground effect: wind tunnel and road conditions, AIAA Paper 95-1909, 1995.
[14] R. Ranzenbach, J.B. Barlow, Cambered aerofoil in ground effect, an experimental and computational study, Society of Automotive Paper No. 96-0909, 1996.
[15] M.R. Ahmed, Y. Kohama, Experimental investigation on the aerodynamic characteristics of a tandem wing configuration in close ground proximity, JSME Int. J. 42 (4) (1999) 612–618.
[16] X. Zhang, J. Zerihan, A. Ruhrmann, M. Deviese, Tip vortices generated by a wing in ground effect, in: Proceedings of the 11th International Symposium on Applications of Laser Techniques to Fluid Mechanics, Portugal, 2002.
[17] J. Zerihan, X. Zhang, Aerodynamics of a single element wing in ground effect, J. Aircraft 37 (6) (2000) 1058–1064.
[18] X. Zhang, J. Zerihan, Turbulent wake behind a single element wing in ground effect, in: Proceedings of the 11th International Symposium on Applications of Laser Techniques to Fluid Mechanics, Portugal, 2002.
[19] N.A. Ahmed, J. Goonaratne, Lift augmentation of a low-aspect-ratio thick wing in ground effect, J. Aircraft 39 (2) (2002) 381–384.
[20] J.B. Barlow, W.H. Rae, A. Pope, Low-Speed Wind Tunnel Testing, third ed., John Wiley, New York, 1999, p. 360 and 374.
[21] F.E. Jørgensen, How to measure turbulence with hot-wire anemometers—a practical guide, Dantec Dyn. (2002) 32–44.
[22] M. Drela, XFOIL: An analysis and design system for low Reynolds number airfoils in low Reynolds number aerodynamics Lecture Notes in Engineering, vol. 54, Springer-Verlag, 1989.
[23] M.S. Shin, Model test of wing-in-ground effect ship, J. Ship Ocean Eng. 29 (2000) 1–5.
[24] R.E. Sheldahl, P.C. Klimas, Aerodynamic characteristics of seven airfoil sections through 180 degrees angle of attack for use in aerodynamic analysis of vertical axis wind turbines, SAND80-2114, Sandia National Laboratories, Albuquerque, New Mexico, 1981.
[25] M.R. Ahmed, G.M. Imran, S.D. Sharma, Experimental investigation of the effect of camber on the aerodynamic characteristics of airfoils in ground effect, ASME Paper No. FEDSM2003-45573, 2003.